$\alpha + {}^{28}$Si and ^{16}O + ^{16}O molecular states and their isoscalar monopole strengths

Masaaki Kimura[1,2,3,*] and Yasutaka Taniguchi[4,3,†]

[1]*Department of Physics, Hokkaido University, Sapporo 060-0810, Japan*
[2]*Nuclear Reaction Data Centre (JCPRG), Hokkaido University, Sapporo 060-0810, Japan*
[3]*Research Center for Nuclear Physics (RCNP), Osaka University, Ibaraki 567-0047, Japan*
[4]*Department of Information Engineering, National Institute of Technology (KOSEN), Kagawa College, Mitoyo 769-1192, Japan*

(Received 20 May 2020; accepted 3 August 2020; published 19 August 2020)

The properties of the $\alpha + {}^{28}$Si and ^{16}O + ^{16}O molecular states, which are embedded in the excited states of ^{32}S and can have an impact on the stellar reactions, are investigated using antisymmetrized molecular dynamics. From the analysis of the cluster spectroscopic factors, the candidates of $\alpha + {}^{28}$Si and ^{16}O + ^{16}O molecular states are identified close to and above the cluster threshold energies. The calculated properties of $\alpha + {}^{28}$Si molecular states are consistent with those reported by $\alpha + {}^{28}$Si resonant scattering experiments. On the other hand, the ^{16}O + ^{16}O molecular state, which is predicted to be identical to the superdeformation of ^{32}S, is inconsistent with the assignment proposed by an α inelastic scattering experiment. Our calculation suggests that the monopole transition from the ground state to the ^{16}O + ^{16}O molecular state is rather weak and is not strongly excited by α inelastic scattering.

DOI: 10.1103/PhysRevC.102.024325

I. INTRODUCTION

The $\alpha + {}^{28}$Si and ^{16}O + ^{16}O molecular states [1–5] that are embedded in the excited states of ^{32}S are fascinating subjects in nuclear cluster physics and nuclear astrophysics. The α-induced reactions such as ^{28}Si$(\alpha,\gamma)^{32}$S and ^{28}Si$(\alpha,p)^{31}$P play an important role in the silicon burning process of the stellar evolution and nucleosynthesis [6]. The $\alpha + {}^{28}$Si molecular states, if they exist at the incident energy, increase the reaction rate in order of magnitude and determine the reaction products [7–9]. In a similar manner, the ^{16}O + ^{16}O molecular states crucially affect the oxygen burning process [10–18]. Furthermore, the ^{16}O + ^{16}O molecular states have unique and interesting characteristics from the view point of nuclear cluster physics. Many theoretical studies [19–26] have predicted that an ^{16}O + ^{16}O molecular band should exist just below the ^{16}O + ^{16}O threshold energy, and it must be identical to the superdeformed state of ^{32}S. Although the superdeformation of ^{32}S has not been observed, the theoretical prediction sheds a new light on the clustering of light nuclei.

Experimentally, these molecular states have been explored using the ordinary techniques such as transfer reactions [27–32] and resonant scattering [33–37]. However, as the molecular states are embedded in the continuum of ^{32}S, it is difficult to identify them from many other resonances. This difficulty prevents us from the full understanding of the molecular states and the superdeformation.

In this decade, instead of the ordinary experimental techniques, the isoscalar monopole and dipole transitions induced by α inelastic scattering are attracting a lot of research interest to overcome the abovementioned problem. These transitions can populate the deep subbarrier resonances and have unique selectivity for molecular states; hence, they are effective to identify the molecular states embedded in the continuum [38–41]. In particular, the method has already been successfully applied to the discussion of clustering and molecular states in many stable and unstable nuclei [42–55]. In the same line of physics, Itoh *et al.* [56] have measured the isoscalar transitions of ^{32}S, identified several excited states with enhanced transition strengths, and proposed a new band assignment for the $\alpha + {}^{28}$Si and ^{16}O + ^{16}O molecular states (and hence the superdeformed states of ^{32}S).

In this work, motivated by the new and interesting experimental data, we theoretically investigated the $\alpha + {}^{28}$Si and ^{16}O + ^{16}O molecular states and their monopole strengths. The framework of antisymmetrized molecular dynamics (AMD) [57–59] has already been applied to the study of the molecular states and superdeformation of *sd*-*pf* nuclei [21,60–63]. Recently it has been extended to handle the rotation effect of the deformed clusters and successfully applied to investigate the ^{12}C + ^{16}O molecular states at deep subbarrier energy [64]. Following these studies, we extended our research, considering both the $\alpha + {}^{28}$Si and ^{16}O + ^{16}O channels in addition to the rotation effect of the deformed ^{28}Si cluster. It was found that the monopole transition has a strong selectivity to $\alpha + {}^{28}$Si molecular states, but it is insensitive to ^{16}O + ^{16}O molecular states. Consequently, we conclude that many of the excited states reported by Itoh *et al.* [56] should be attributed to the $\alpha + {}^{28}$Si molecular states. From the systematics of the cluster spectroscopic factors and $B(E2)$ transition strengths, we also propose the assignment of the $\alpha + {}^{28}$Si and ^{16}O + ^{16}O molecular bands.

*masaaki@nucl.sci.hokudai.ac.jp
†taniguchi-y@di.kagawa-nct.ac.jp

This paper is organized as follows. In the next section, we explain the AMD framework and how we handle both the $\alpha + {}^{28}$Si and ${}^{16}\mathrm{O}+{}^{16}\mathrm{O}$ channels, as well as the rotation effect of the deformed ^{28}Si cluster. In Sec. III, we explain the $\alpha + {}^{28}$Si and ${}^{16}\mathrm{O}+{}^{16}\mathrm{O}$ wave functions obtained by the variational calculations. We discuss the properties of the 0^+ states and their monopole strengths in comparison with the observations. We also suggest the $\alpha + {}^{28}$Si and ${}^{16}\mathrm{O}+{}^{16}\mathrm{O}$ molecular band assignments. The final section summarizes this work.

II. THEORETICAL FRAMEWORK

The theoretical framework used in this paper is the same as that of our previous work for the ${}^{12}\mathrm{C}+{}^{16}\mathrm{O}$ molecular states. Deformed-basis AMD is combined with the d-constraint method. The Hamiltonian is expressed as

$$H = \sum_{i=1}^{A} t(i) + \sum_{i<j}^{A} v_{NN}(ij) + \sum_{i<j}^{A} v_C(ij) - t_{\mathrm{c.m.}}, \quad (1)$$

where the Gogny D1S parameter set [65] is used for the effective nucleon-nucleon interaction v_{NN} and the Coulomb interaction v_C is approximated by a sum of seven Gaussians. The center-of-mass kinetic energy $t_{\mathrm{c.m.}}$ is properly removed from the Hamiltonian without any approximation. This Hamiltonian reasonably describes the threshold energies of interest without any adjustment. The $\alpha + {}^{28}$Si and ${}^{16}\mathrm{O}+{}^{16}\mathrm{O}$ threshold energies measured from the ^{32}S ground state are calculated as 7.56 and 16.25 MeV, respectively, which are compared with the experimental data of 6.95 and 16.54 MeV.

The variational wave function of deformed-basis AMD is a parity-projected Slater determinant of the single-particle wave packets [66]:

$$\Phi = \mathcal{A}\{\varphi_1, \ldots, \varphi_A\}, \quad (2)$$

$$\varphi_i = \prod_{\sigma=x,y,z} \left(\frac{2\nu_\sigma}{\pi}\right)^{1/4} \exp\{-\nu_\sigma(r_\sigma - Z_{i\sigma})^2\} \times (\alpha_i |\xi_\uparrow\rangle + \beta_i |\xi_\downarrow\rangle)(|p\rangle \text{ or } |n\rangle), \quad (3)$$

where each of the φ_i has the deformed Gaussian form and has the following parameters: the centroid of the Gaussian $\boldsymbol{Z}_i$, size parameter $\boldsymbol{\nu}$, and spin directions α_i and β_i. The isospin part is fixed to either protons or neutrons. The size parameter $\boldsymbol{\nu}$ is a real-valued vector, but the other parameters are complex-valued. They are determined by the energy variation with two different constraints. The first one is the constraint on the quadrupole deformation parameter β, which we call the β constraint. It is noted that the β constraint was already used to study the superdeformation of ^{32}S and the ${}^{16}\mathrm{O}+{}^{16}\mathrm{O}$ molecular states within the AMD framework [21]. The second constraint is imposed on the intercluster distance between the α and ^{28}Si clusters, and between two ^{16}O clusters, which we call the d constraint [67]. We classify the centroids of the wave packets into two groups corresponding to the cluster configurations, and we define an approximate intercluster distance d as the distance between the center-of-masses of two groups. For example, d for the $\alpha + {}^{28}$Si configuration is defined as

$$d = \left| \frac{1}{4} \sum_{i\in\alpha} \mathrm{Re}\boldsymbol{Z}_i - \frac{1}{28} \sum_{i\in{}^{28}\mathrm{Si}} \mathrm{Re}\boldsymbol{Z}_i \right|. \quad (4)$$

The value of d is constrained from 2 to 8 fm with the interval of 0.5 fm. It is emphasized that the d constraint is essential for describing the $\alpha + {}^{28}$Si molecular states, because the β constraint yields only the mean-field and ${}^{16}\mathrm{O}+{}^{16}\mathrm{O}$ molecular states. Furthermore, it can handle the cluster polarization effect and the rotation effect of the deformed clusters in a natural manner.

From the energy variation with the constraints, we obtain the wave functions that have the minimum energies for each given value of β or d. After the energy variation, the wave functions are projected to the eigenstates of the angular momentum and superposed to diagonalize the Hamiltonian (generator coordinate method, GCM):

$$\Psi^{J\pi}_{M\alpha} = \sum_{iK} b_{iK\alpha} P^J_{MK} \Phi^\pi(\beta_i) + \sum_{iK} d_{iK\alpha} P^J_{MK} \Phi^\pi(d_i), \quad (5)$$

where P^J_{MK} denotes the angular momentum projector, $\Phi^\pi(\beta_i)$ and $\Phi^\pi(d_i)$ are the wave functions obtained by the β constraint and the d constraint, respectively. The coefficients of the superposition b_{iK} and d_{iK} are determined by solving the Hill-Wheeler equation [68].

As a measure for the $\alpha + {}^{28}$Si and ${}^{16}\mathrm{O}+{}^{16}\mathrm{O}$ clustering, we calculate the reduced width amplitude (RWA), which is the probability amplitude to find the clusters at the intercluster distance a. It is defined as the overlap between the reference-cluster wave function and the GCM wave function given by Eq. (5),

$$y_\ell(a) = \sqrt{\frac{32!}{C_1!C_2!}} \left\langle \frac{\delta(r-a)}{r^2} \left[\Phi_{C_1}\Phi_{C_2}Y_\ell(\hat{r})\right]^J_M \middle| \Psi^{J\pi}_{M\alpha} \right\rangle, \quad (6)$$

where $C_{1,2}$ and Φ_{C_1,C_2} denote the masses and wave functions of clusters, respectively: $C_1 = 4$ and $C_2 = 28$ for the $\alpha + {}^{28}$Si configurations, and $C_1 = C_2 = 16$ for the ${}^{16}\mathrm{O}+{}^{16}\mathrm{O}$ configurations. The reference wave function (bra state) describes the system in which two clusters with the masses of C_1 and C_2 are mutually orbiting with the angular momentum ℓ and the intercluster distance a. Here, the wave functions of the α and ^{16}O clusters are assumed to be the the harmonic oscillator wave functions with the doubly closed shell structure, which reproduce the observed charge radii. The wave function of the ^{28}Si cluster is approximated using a single AMD wave function projected to either the $J^\pi = 0^+$ state or the $J^\pi = 2^+$ state. Equation (6) was calculated using the Laplace expansion method [69] for the $\alpha + {}^{28}$Si channel and using the projection method to the Brink wave function [70,71] for the ${}^{16}\mathrm{O}+{}^{16}\mathrm{O}$ channel. The cluster spectroscopic factors in these channels are calculated by the squared integral of y_ℓ:

$$S_\ell = \int_0^\infty da\, a^2 |y_\ell(a)|^2, \quad (7)$$

which is enhanced for the developed cluster states and is used to identify the molecular states.

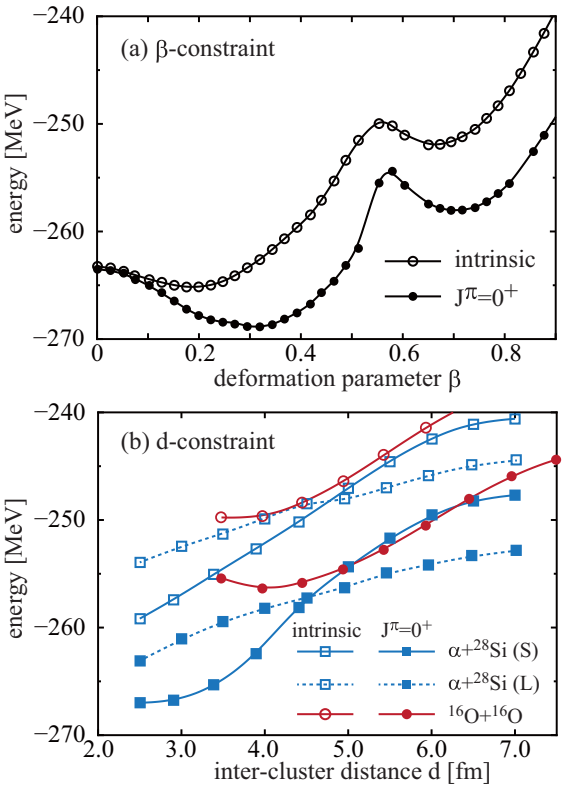

FIG. 1. Energy curves of the positive-parity states before (intrinsic) and after the angular momentum projection to $J^\pi = 0^+$. (a) The energy curves obtained by the constraint on the quadrupole deformation parameter β. (b) The energy curves of the $\alpha + {}^{28}$Si and ^{16}O + ^{16}O molecular configurations.

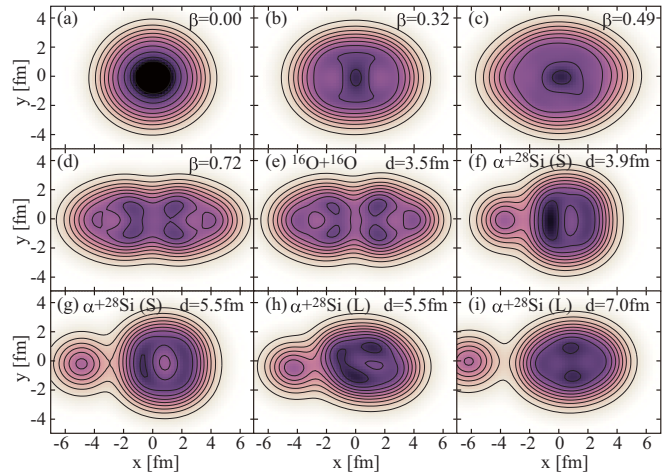

FIG. 2. (a)–(d) The intrinsic densities obtained by the β constraint. Panels (b) and (d) correspond to the ground and superdeformed minima on the energy surface, respectively. (e)–(i) The intrinsic densities obtained by the d constraint. Panel (e) shows the intrinsic density of the ^{16}O + ^{16}O configuration at the energy minimum. Panels (f) and (g) are the S-type $\alpha + {}^{28}$Si configurations in which the symmetry axis of the ^{28}Si cluster is parallel to the x axis, while panels (h) and (i) are the L-type configurations in which the shortest axis is perpendicular to the x axis.

In this work, we focus on the isoscalar monopole (IS0) transition strength, which has been regarded and utilized as a novel probe for the molecular states in stable and unstable nuclei. The transition operator is defined as follows:

$$\mathcal{M}^{\mathrm{IS0}} = \sum_{i=1}^{A} r_i'^2. \tag{8}$$

Note that the single-particle coordinate $\boldsymbol{r}_i'$ is measured from the center-of-mass $\boldsymbol{r}_{\mathrm{c.m.}}$, i.e., $\boldsymbol{r}_i' \equiv \boldsymbol{r}_i - \boldsymbol{r}_{\mathrm{c.m.}}$; hence, our calculation is free from the spurious center-of-mass contributions. The reduced transition matrix from the ground state to the excited 0^+ state is calculated as

$$M(\mathrm{IS0}; 0_1^+ \to 0_{\mathrm{ex.}}^+) = \langle \Psi(0_{\mathrm{ex.}}^+) | \mathcal{M}^{\mathrm{IS0}} | \Psi(0_{\mathrm{g.s.}}^+) \rangle \,, \tag{9}$$

where $\Psi(0_{\mathrm{g.s.}}^+)$ and $\Psi(0_{\mathrm{ex.}}^+)$ are the wave functions of the ground and excited 0^+ states, respectively.

III. RESULTS AND DISCUSSIONS

A. Molecular configurations obtained by the variational calculations

Figure 1(a) shows the energy curves of the positive-parity states obtained by the β- constraint. It has two minima at $\beta = 0.32$ and 0.72 after the angular momentum projection, which correspond to the ground state and the superdeformed state, respectively. Their intrinsic density distributions shown in Figs. 2(b) and 2(d) appear considerably different and impress the exotic shape of the superdeformed minimum [Fig. 2(d)], which is extremely deformed with a neck and two-centered. Similar density distributions of the superdeformed state have also been reported by many other theoretical studies [21–26,72–74].

The energy curves for the $\alpha + {}^{28}$Si and ^{16}O + ^{16}O molecular configurations obtained by the d constraint are shown in Fig. 1(b). We have obtained two different $\alpha + {}^{28}$Si molecular configurations that have different orientations of the deformed ^{28}Si cluster. We call them S- and L-type configurations in the following. In the S-type configuration denoted by (S), the symmetry axis of the oblate deformed ^{28}Si cluster is parallel to the x axis on which the centers of mass of α and ^{28}Si clusters are placed [see Figs. 2(f) and 2(g)]. On the contrary, in the L-type configuration (L), the symmetry axis of ^{28}Si is perpendicular to the x axis [see Figs. 2(h) and 2(i)]. By mixing both the S- and L-type configurations, we can handle the rotation effect of the deformed ^{28}Si cluster within the AMD framework. It is also noted that these two configurations have different single-particle structures at a small intercluster distance. The S-type configuration approaches the ground-state configuration ($0\hbar\omega$) at a short intercluster distance; hence, its energy ($E = -267.0$ MeV at $d = 2.5$ fm) is close to that of the ground-state minimum ($E = -268.9$ MeV at $\beta = 0.25$) as shown in Fig. 1. It is important to note that the squared overlaps of the wave functions between the ground-state and the S-type $\alpha + {}^{28}$Si configurations are non-negligible after the parity and angular-momentum projection to $J^\pi = 0^+$, although they appear quite different at a glance. Indeed, the overlap between the wave functions shown in Figs. 2(b)

and 2(f) is as large as 0.45. On the contrary, the L-type configuration approaches a $4\hbar\omega$ excited configuration at a small distance. Consequently, the L-type configurations are orthogonal to the ground-state configuration and their energies are relatively higher than those of the S-type configurations. It is noted that these different asymptotics of the molecular configurations play a crucial role in the isoscalar monopole transitions.

The $^{16}\mathrm{O}+^{16}\mathrm{O}$ configuration is almost identical to the superdeformed state (a $4\hbar\omega$ configuration) at the energy minimum ($d = 3.5$ fm), and its energy (-257.6 MeV) is very close to that of the superdeformed minimum (-258.0 MeV). It is impressive that their density distributions are significantly similar to each other [Figs. 2(d) and 2(e)], and the squared overlap of their wave functions is as large as 0.92, which indicates that they are actually identical. This is the reason why many theoretical studies [20–26,72] discuss the similarity of the superdeformation of ^{32}S and the $^{16}\mathrm{O}+^{16}\mathrm{O}$ molecular states. However, despite the consistent and convincing discussions by many theories, experimental information about the superdeformation of ^{32}S had been rather limited [32,75]. Recently, Itoh *et al.* [56] provided a new report by investigating the isoscalar monopole transition strengths of ^{32}S. In particular, based on the observed strong monopole transitions, they proposed a new assignment of the $^{16}\mathrm{O}+^{16}\mathrm{O}$ molecular states, and hence the superdeformed states. We verify their assignment in the following sections.

B. Molecular states and their monopole strengths

In this section, we focus on the $J^\pi = 0^+$ states and discuss their molecular structure, monopole transition strengths, and experimental candidates. However, before the discussion of the present results, it may be useful to summarize the experimental information about the $\alpha + {}^{28}$Si and $^{16}\mathrm{O}+^{16}\mathrm{O}$ molecular states. Many resonances that are the candidates of the $\alpha + {}^{28}$Si molecular states have been reported above the $\alpha + {}^{28}$Si threshold energy by the resonant scattering experiments [34–37]. In particular, Lönnroth *et al.* [37] comprehensively summarized the observed resonances covering a broad energy region and proposed an $\alpha + {}^{28}$Si molecular band. The candidates of the 0^+ resonances they proposed are fragmented into many states in between 10.25 and 11.05 MeV as shown in Fig. 3. They all have the α-decay widths ranging from a few keV to a few tens of keV, and many of them coincide with the resonances observed in other experiments [34–36]. The α-transfer reaction [27–31] is another useful probe for the $\alpha + {}^{28}$Si molecular states, especially for the states below the decay threshold. Peng *et al.* [29,30] and Tanabe *et al.* [31] reported the α spectroscopic factor of the 0^+_2 states by means of the (^{16}O, ^{12}C) and (^{6}Li, d) reactions, respectively. They concluded that the α spectroscopic factor of the 0^+_2 state is approximately 0.50–0.75 relative to that of the ground state (it varies, depending on the incident energy). Tanabe *et al.* [31] also reported that several states at 10 to 11 MeV are strongly populated by the (^{6}Li, d) reaction and hence are suggested as the candidates of the $\alpha + {}^{28}$Si molecular states. Although the spin-parity assignment was not discussed, it is important to note that the energies of these states are very close to the 0^+ resonances reported by Lönnroth *et al.* [37].

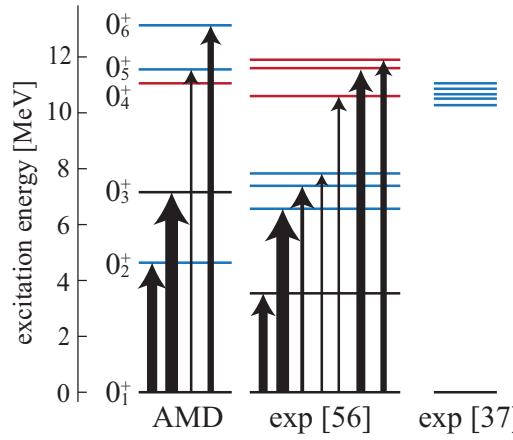

FIG. 3. The calculated and observed [37,56] candidates of the $\alpha + {}^{28}$Si (blue lines) and $^{16}\mathrm{O}+^{16}\mathrm{O}$ (red lines) molecular states with $J^\pi = 0^+$. The widths of the arrows are proportional to the isoscalar monopole transition matrix.

The isoscalar monopole strength is a novel probe for the molecular states and has a unique selectivity. Itoh *et al.* [56] measured the isoscalar monopole transitions of ^{32}S by the α inelastic scattering and reported several states as the candidates of the molecular states. In addition to the 0^+_2 state, they found that six excited states have enhanced monopole strength as listed in Table I. They are classified into two groups; three states at 6 to 8 MeV and the other three at 10 to 12 MeV. As summarized in Fig. 3, the former group was proposed as the $\alpha + {}^{28}$Si molecular states, and the latter as the $^{16}\mathrm{O}+^{16}\mathrm{O}$ molecular states. Furthermore, the latter group, the states at 10 to 12 MeV, is also proposed as the superdeformed states, because the $^{16}\mathrm{O}+^{16}\mathrm{O}$ molecular state and the superdeformation should be identical. To summarize the experimental data, the 0^+ resonances at 10 to 12 MeV are observed in many experiments. They are assigned as

TABLE I. The calculated excitation energies in MeV, isoscalar monopole transition matrices in fm^2, and cluster spectroscopic factors of the 0^+ states. $S_{\alpha\ell=0}$, $S_{\alpha\ell=2}$, and S_{O} denote the spectroscopic factors in the $\alpha + {}^{28}\mathrm{Si}(0^+_1)$, $\alpha + {}^{28}\mathrm{Si}(2^+_1)$, and $^{16}\mathrm{O}+^{16}\mathrm{O}$ channels, respectively. The observed excitation energies and the isoscalar monopole matrices [56] are also listed.

	AMD					Expt.	
	E_x	M(IS0)	$S_{\alpha,\ell=0}$	$S_{\alpha,\ell=2}$	S_{O}	E_x	M(IS0)
0^+_1	0.0		0.09	0.04	0.00	0.0	
0^+_2	4.6	5.7	0.05	0.06	0.00	3.78	4.0
0^+_3	7.0	6.5	0.02	0.01	0.02	6.59	6.3
						7.65	3.8
						7.95	2.7
0^+_4	11.0	0.0	0.02	0.01	0.32		
0^+_5	11.6	2.8	0.29	0.14	0.00	10.49	3.3
0^+_6	13.1	4.8	0.34	0.12	0.02	11.62	5.4
						11.90	4.3

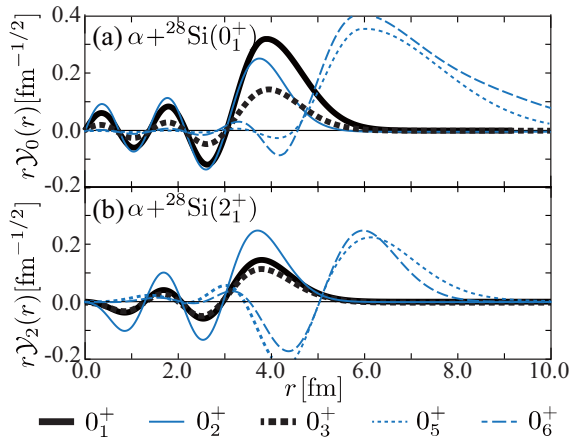

FIG. 4. The reduced width amplitudes in the $\alpha + {}^{28}$Si(0^+_1) and $\alpha + {}^{28}$Si(2^+_1) channels calculated for the 0^+_1, 0^+_2, 0^+_3, 0^+_5, and 0^+_6 states, respectively.

the $\alpha + {}^{28}$Si molecular states in Refs. [31,34–37], but are assigned as the ^{16}O + ^{16}O molecular states in Ref. [56]. Itoh *et al.* also reported another group of the states at 6 to 8 MeV and assigned them as the $\alpha + {}^{28}$Si molecular states.

Now, we discuss the present numerical results in comparison with the abovementioned experimental data. The calculated ground state is predominated by the mean-field configuration shown in Fig. 2(b). The squared overlap between the ground state and this configuration is 0.92. It is noted that the ground state also has a large overlap with the S-type $\alpha + {}^{28}$Si molecular configurations with small intercluster distances. The overlap between the ground state and the $\alpha + {}^{28}$Si configuration shown in Fig. 2(f) is as large as 0.46, and the calculated spectroscopic factors of the ground state are $S_\alpha = 0.09$ and 0.04 in the $\alpha + {}^{28}$Si(0^+_1) and $\alpha + {}^{28}$Si(2^+_1) channels, respectively. This small amount of the cluster component in the ground state can be explained by the Bayman-Bohr theorem [76], which proves the identity of SU(3) shell-model wave functions and corresponding cluster wave functions with zero intercluster distance. In other words, the theorem guarantees that even a pure shell-model-like structure contains a certain amount of the cluster component. In fact, the calculated RWA of the ground state (Fig. 4) has a small peak at 3 to 4 fm showing non-negligible α cluster formation at the nuclear surface. These results qualitatively agree with the observed cross section of ^{32}S(p, $p\alpha$)^{28}Si [77], which is sensitive to the α cluster formation at the surface of the ground state [78–82]. On the other hand, the ground state has no overlap with the L-type $\alpha + {}^{28}$Si and ^{16}O + ^{16}O configurations because they asymptotically approach the $4\hbar\omega$ excited configurations at zero intercluster distance and are almost orthogonal to the ground state.

The 0^+_2 state largely consists of the almost spherical configuration shown in Fig. 2(a), and the squared overlap is 0.67. In addition, it also has a non-negligible overlap with the S-type $\alpha + {}^{28}$Si molecular configuration. The overlap between the 0^+_2 state and the $\alpha + {}^{28}$Si configuration shown in Fig. 2(f) is 0.22, which can also be explained by the Bayman-Bohr theorem. The calculated RWA and α spectroscopic factors are not as large as those of the ground state, and the ratio of S_α to the ground state is $S_{\alpha,\ell=0}(0^+_2)/S_{\alpha,\ell=0}(0^+_1) = 0.56$. This reduction of S_α relative to the ground state reasonably agrees with the observed values which are in between 0.51 and 0.75 [29–31]. It is noted that these small α cluster components in the ground and 0^+_2 states enlarge the monopole transition strength (5.7 fm^2) between these states. If we exclude the $\alpha + {}^{28}$Si molecular configurations from the GCM calculation, the spectroscopic factors of the ground and 0^+_2 states are reduced to 0.05 and 0.02 in the $\alpha + {}^{28}$Si(0^+_1) channel, and the monopole transition matrix is reduced to 2.32 fm^2, which is smaller than the observed value of 4.0 fm^2.

The 0^+_3 state has the largest overlap with the configuration shown in Fig. 2(c), which amounts to 0.36. This state has similar magnitude of the overlap with many other configurations on the β-constraint energy surface shown in Fig. 1(a), but it scarcely overlaps with the molecular configurations. Therefore, its RWA and spectroscopic factors are small, and we conclude that the 0^+_3 state is a β-vibration state. This interpretation explains the large monopole strength of this state, as it is well known that the β vibration also enhances the monopole transition strengths [83]. Itoh *et al.* [56] observed three 0^+ states (6.59, 7.65, and 7.95 MeV states) with enhanced monopole strengths in this energy region, and the 6.59 MeV state plausibly coincides with the calculated 0^+_3 state. However, neither of calculation nor other experiments reported additional 0^+ states in between 6 to 8 MeV [84]. Therefore, more detailed study is needed to confirm the 7.65 and 7.95 MeV states.

The 0^+_4 state is the superdeformed state that was already discussed in the previous AMD study [21]. It has the large squared overlap (0.95) with the configuration shown in Fig. 2(d). In addition, it also has large overlap with the ^{16}O + ^{16}O configuration shown in Fig. 2(e), which amounts to 0.92. Hence, the superdeformed state of ^{32}S is regarded as an ^{16}O + ^{16}O molecular state; i.e., it has a duality of the superdeformation and clustering. From the observed strong monopole transitions, Itoh *et al.* [56] proposed the 10.49, 11.62, and 11.90 MeV states as the superdeformed states. However, in contrast to their assignment, the present calculation shows that the monopole transition to the superdeformed state is negligible. This result clearly reflects the nature of the monopole transition. As explained by Yamada *et al.* [40], the monopole transition excites the molecular configurations that are contained in the ground state. In other words, the molecular configurations orthogonal to the ground state at zero intercluster distance are not populated by the monopole transition. Because the ^{16}O + ^{16}O configuration is orthogonal to the ground state, the monopole transition from the ground state to the ^{16}O + ^{16}O molecular state is strictly forbidden. Therefore, the present result does not support the assignment of the ^{16}O + ^{16}O molecular state and the superdeformed state observed in the α inelastic scattering experiment.

The 0^+_5 and 0^+_6 states are the highly excited $\alpha + {}^{28}$Si molecular states that overlap with both the S- and L-type $\alpha + {}^{28}$Si configurations shown in Figs. 2(f)–2(i). As seen in Table I, these states are predominated by the $\alpha + {}^{28}$Si(0^+_1) channel, while the ground state and the 0^+_2 state are the mixture of the $\alpha + {}^{28}$Si(0^+_1) and $\alpha + {}^{28}$Si(2^+_1) channels. This

is because of the weak interaction between the clusters in the 0_5^+ and 0_6^+ states, which deexcites the ^{28}Si cluster to its ground state (weak cluster polarization). Note that the RWA of the 0_5^+ and 0_6^+ states has a peak at approximately 6 fm, which indicates the large intercluster distance and enhanced clustering. Owing to this pronounced $\alpha + {}^{28}$Si molecular structure, these states have large monopole transition strengths, and they may correspond to any of the 10.49, 11.62, and 11.90 MeV states observed by Itoh *et al.* [56]. Interestingly, the $\alpha + {}^{28}$Si molecular states observed by Lönnroth *et al.* [37] are located at the same energy region, and we consider that they are the same $\alpha + {}^{28}$Si molecular states. We also comment on the magnitude of the calculated S_α for these states. Despite the large overlap with the pronoucned $\alpha + {}^{28}$Si configurations, the calculated spectroscopic factor for the $\alpha + {}^{28}\mathrm{Si}(0_1^+)$ channel is not so large. This is due to the following two reasons. The first is the deformation and polarization of the ^{28}Si cluster induced by the interaction with the α cluster. Because of this, the spectroscopic factor is distributed to various inelastic channels $\alpha + {}^{28}\mathrm{Si}^*$. The second is the coupling with other noncluster configurations. Because of this coupling the spectroscopic factor is fragmented into many states as experimentally reported by Lönnroth *et al.* [37].

Thus, the present calculation has revealed the characteristics of the excited 0^+ states. The monopole transition from the ground state has a selectivity, because the ground state is a mixture of the deformed mean-field and $\alpha + {}^{28}$Si molecular structure. The β-vibration state and $\alpha + {}^{28}$Si molecular states are strongly excited, but the $^{16}\mathrm{O} + {}^{16}\mathrm{O}$ molecular state (and hence the superdeformed state) is not. We conclude that many of the states with enhanced monopole strengths observed below 12 MeV should be attributed to the $\alpha + {}^{28}$Si molecular states.

C. Assignment of the rotational bands

Figure 5 shows our assignment of the $\alpha + {}^{28}$Si and $^{16}\mathrm{O} + {}^{16}\mathrm{O}$ molecular bands from the present calculation. The assignment is based on the calculated spectroscopic factors. That is, if the spectroscopic factors in the $^{16}\mathrm{O} + {}^{16}\mathrm{O}$ channel or if the sum of the spectroscopic factors in the $\alpha + {}^{28}\mathrm{Si}(0_1^+)$ and $\alpha + {}^{28}\mathrm{Si}(2_2^+)$ channels is larger than 0.10, we have assigned the state as the molecular state. The figure also shows the $B(E2\uparrow)$ strengths larger than 150 e^2 fm^4, which confirms that most of the molecular states are connected by the strong $B(E2)$ transitions due to their strong quadrupole deformation.

The assignment of the $^{16}\mathrm{O} + {}^{16}\mathrm{O}$ band is essentially same as that proposed in the previous AMD study and rather unique as it does not strongly fragment into many states. The lowest $^{16}\mathrm{O} + {}^{16}\mathrm{O}$ band is built on the 0_4^+ state at 11.0 MeV, and as already discussed in Ref. [21], it is identical to the superdeformed band with huge moment-of-inertia as large as $\hbar^2/(2\mathcal{I}) = 68$ keV. Another $^{16}\mathrm{O} + {}^{16}\mathrm{O}$ molecular band, in which the relative motion between ^{16}O clusters is excited, exists at approximately $E_x = 20$ MeV, and the member states of this band with $J \geqslant 2$ are fragmented into two or three states.

The assignment of the $\alpha + {}^{28}$Si band is not as unique as the $^{16}\mathrm{O} + {}^{16}\mathrm{O}$ case because the member states are fragmented into many states due to the strong coupling of the

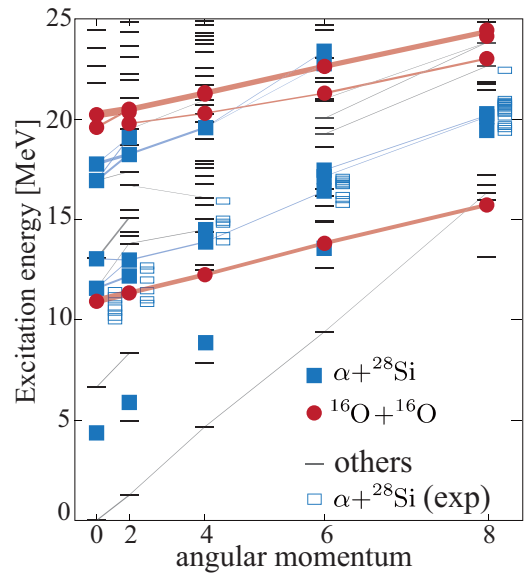

FIG. 5. The calculated molecular bands up to $J^\pi = 8^+$ states. The solid squares and circles show the $\alpha + {}^{28}$Si and $^{16}\mathrm{O} + {}^{16}\mathrm{O}$ molecular states, respectively. The open squares show the observed candidates of the $\alpha + {}^{28}$Si molecular band [37]. The $B(E2\uparrow)$ transitions stronger than 150 e^2 fm^4 are shown by the connecting lines whose widths are proportional to the magnitude of the transition matrices.

$\alpha + {}^{28}\mathrm{Si}(0_1^+)$ and $\alpha + {}^{28}\mathrm{Si}(2_2^+)$ channels, as well as to the coupling with the noncluster configurations. There are many states that have small but non-negligible spectroscopic factors in the $\alpha + {}^{28}$Si channels. For example, the states that have spectroscopic factors larger than 0.05 are almost twice as many as those shown in Fig. 5. This result is consistent with the observation by Lönnroth *et al.* [37] who reported many excited states that have a small fraction of the $\alpha + {}^{28}$Si spectroscopic factors. However, for the sake of clarity and simplicity, here, we discuss the states with sufficiently large spectroscopic factors (larger than 0.10). We suggest an $\alpha + {}^{28}$Si band built on the 0_5^+ and 0_6^+ states. Although the member states are considerably fragmented, it can be confirmed that many states are connected by the strong $B(E2)$ transitions. We consider that this band corresponds to the $\alpha + {}^{28}$Si band reported by Lönnroth *et al.* [37] as the energies of the member states plausibly agree with their observation. We also comment that the other band, in which the relative motion of the clusters is excited, may be built on the 0^+ states approximately at 17 MeV. We can see the candidates of the band member states up to $J^\pi = 6^+$, although the fragmentation is rather strong. Experimentally, several candidates of the $\alpha + {}^{28}$Si states have been reported above 15 MeV without firm spin-parity assignment [85,86], and the present results may explain these observations.

IV. SUMMARY

We have investigated the properties of the $\alpha + {}^{28}$Si and $^{16}\mathrm{O} + {}^{16}\mathrm{O}$ molecular states in the ^{32}S excited states. An extended framework of AMD has been applied for handling

both of the $\alpha + {}^{28}$Si and ^{16}O + ^{16}O channels in addition to the rotation effect of the deformed ^{28}Si cluster. It was found that the isoscalar monopole transition has strong selectivity in the molecular states: It strongly excites the $\alpha + {}^{28}$Si molecular states, but is inactive in the ^{16}O + ^{16}O molecular states. This selectivity originates in the different asymptotic behavior of the molecular configurations at zero intercluster distance. We found that the assignment of the $\alpha + {}^{28}$Si molecular states proposed by Lönnroth *et al.* [37] reasonably agrees with the present calculation, while the ^{16}O + ^{16}O molecular state or the superdeformed state proposed by Itoh *et al.* [56] does not, because the monopole transition strengths of the ^{16}O + ^{16}O molecular states are rather weak and are not excited strongly by the α inelastic scattering.

ACKNOWLEDGMENTS

This work was supported by a grant for the RCNP joint research project, the collaborative research program 2020 at Hokkaido University, and Japan Society for the Promotion of Science (JSPS) Grant No. JP 19K03859.

[1] D. Baye and G. Reidemeister, Nucl. Phys. A **258**, 157 (1976).
[2] T. Ando, K. Ikeda, and A. Tohsaki-Suzuki, Prog. Theor. Phys. **64**, 1608 (1980).
[3] D. Baye and P. Descouvemont, Nucl. Phys. A **419**, 397 (1984).
[4] K. Langanke, R. Stademann, and D. Frekers, Phys. Rev. C **29**, 40 (1984).
[5] Y. Kondo, B. A. Robson, and R. Smith, Phys. Lett. B **227**, 310 (1989).
[6] D. Bodansky, D. D. Clayton, and W. A. Fowler, Phys. Rev. Lett. **20**, 161 (1968).
[7] P. J. Smulders, Physica **30**, 1197 (1964).
[8] J. W. Toevs, Nucl. Phys. A **172**, 589 (1971).
[9] D. W. Rogers, W. R. Dixon, and R. S. Storey, Nucl. Phys. A **281**, 345 (1977).
[10] H. Spinka and H. Winkler, Nucl. Phys. A **233**, 456 (1974).
[11] D. G. Kovar, D. F. Geesaman, T. H. Braid, Y. Eisen, W. Henning, T. R. Ophel, M. Paul, K. E. Rehm, S. J. Sanders, P. Sperr, J. P. Schiffer, S. L. Tabor, S. Vigdor, B. Zeidman, and F. W. Prosser, Phys. Rev. C **20**, 1305 (1979).
[12] G. Hulke, C. Rolfs, and H. P. Trautvetter, Z. Phys. A: At. Nucl. **297**, 161 (1980).
[13] S. C. Wu and C. A. Barnes, Nucl. Phys. A **422**, 373 (1984).
[14] J. Thomas, Y. T. Chen, S. Hinds, D. Meredith, and M. Olson, Phys. Rev. C **33**, 1679 (1986).
[15] T. A. Weaver and S. E. Woosley, Phys. Rep. **227**, 65 (1993).
[16] M. F. El Eid, B. S. Meyer, and L.-S. The, Astrophys. J. **611**, 452 (2004).
[17] A. Diaz-Torres, L. R. Gasques, and M. Wiescher, Phys. Lett. B **652**, 255 (2007).
[18] L. R. Gasques, E. F. Brown, A. Chieffi, C. L. Jiang, M. Limongi, C. Rolfs, M. Wiescher, and D. G. Yakovlev, Phys. Rev. C **76**, 035802 (2007).
[19] M. Freer, R. R. Betts, and A. H. Wuosmaa, Nucl. Phys. A **587**, 36 (1995).
[20] S. Ohkubo and K. Yamashita, Phys. Rev. C **66**, 021301(R) (2002).
[21] M. Kimura and H. Horiuchi, Phys. Rev. C **69**, 051304(R) (2004).
[22] J. A. Maruhn, M. Kimura, S. Schramm, P.-G. Reinhard, H. Horiuchi, and A. Tohsaki, Phys. Rev. C **74**, 044311 (2006).
[23] T. Ichikawa, Y. Kanada-En'yo, and P. Möller, Phys. Rev. C **83**, 054319 (2011).
[24] J.-P. Ebran, E. Khan, T. Nikšić, and D. Vretenar, Phys. Rev. C **90**, 054329 (2014).
[25] D. Ray and A. V. Afanasjev, Phys. Rev. C **94**, 014310 (2016).
[26] J.-P. Ebran, E. Khan, T. Nikšić, and D. Vretenar, J. Phys. G: Nucl. Part. Phys. **44**, 103001 (2017).
[27] J. V. Maher, K. A. Erb, G. H. Wedberg, J. L. Ricci, and R. W. Miller, Phys. Rev. Lett. **29**, 291 (1972).
[28] R. A. Lindgren, J. P. Trentelman, N. Anantaraman, H. E. Gove, and F. C. Jundt, Phys. Lett. B **49**, 263 (1974).
[29] J. C. Peng, J. V. Maher, M. S. Chiou, W. J. Jordan, F. C. Wang, and M. W. Wu, Phys. Lett. B **80**, 35 (1978).
[30] G. P. A. Berg, M. A. G. Fernandes, K. Nagatani, J. C. Peng, B. Berthier, J. P. Fouan, J. Gastebois, J. P. Le Fèvre, and M.-C. Lemaire, Phys. Rev. C **19**, 62 (1979).
[31] T. Tanabe, M. Yasue, K. Sato, K. Ogino, Y. Kadota, Y. Taniguchi, K. Obori, K. Makino, and M. Tochi, Phys. Rev. C **24**, 2556 (1981).
[32] K. Morita, S. Kubono, M. H. Tanaka, H. Utsunomiya, M. Sugitani, S. Kato, J. Schimizu, T. Tachikawa, and N. Takahashi, Phys. Rev. Lett. **55**, 185 (1985).
[33] M. Gai, E. C. Schloemer, J. E. Freedman, A. C. Hayes, S. K. Korotky, J. M. Manoyan, B. Shivakumar, S. M. Sterbenz, H. Voit, S. J. Willett, and D. A. Bromley, Phys. Rev. Lett. **47**, 1878 (1981).
[34] P. Manngård, Z. Phys. A: Hadrons Nucl. **349**, 335 (1994).
[35] K. M. Källman, V. Z. Goldberg, T. Lönnroth, P. Manngård, A. E. Pakhomov, and V. V. Pankratov, Nucl. Instrum. Methods Phys. Res., Sect. A **338**, 413 (1994).
[36] K.-M. Källman, M. Brenner, V. Z. Goldberg, T. Lönnroth, P. Manngård, A. E. Pakhomov, and V. V. Pankratov, Eur. Phys. J. A **16**, 159 (2003).
[37] T. Lönnroth, M. Norrby, V. Z. Goldberg, G. V. Rogachev, M. S. Golovkov, K. M. Källman, M. Lattuada, S. V. Perov, S. Romano, B. B. Skorodumov, G. P. Tiourin, W. H. Trzaska, A. Tumino, and A. N. Vorontsov, Eur. Phys. J. A **46**, 5 (2010).
[38] T. Kawabata, H. Akimune, H. Fujita, Y. Fujita, M. Fujiwara, K. Hara, K. Hatanaka, M. Itoh, Y. Kanada-En'yo, S. Kishi, K. Nakanishi, H. Sakaguchi, Y. Shimbara, A. Tamii, S. Terashima, M. Uchida, T. Wakasa, Y. Yasuda, H. Yoshida, and M. Yosoi, Phys. Lett. B **646**, 6 (2007).
[39] Y. Kanada-En'yo, Phys. Rev. C **75**, 024302 (2007).
[40] T. Yamada, Y. Funaki, H. Horiuchi, K. Ikeda, and A. Tohsaki, Prog. Theor. Phys. **120**, 1139 (2008).
[41] Y. Chiba, M. Kimura, and Y. Taniguchi, Phys. Rev. C **93**, 034319 (2016).
[42] Y. Funaki, T. Yamada, H. Horiuchi, G. Röpke, P. Schuck, and A. Tohsaki, Phys. Rev. Lett. **101**, 082502 (2008).
[43] M. Ito, Phys. Rev. C **83**, 044319 (2011).

[44] T. Yamada, Y. Funaki, T. Myo, H. Horiuchi, K. Ikeda, G. Röpke, P. Schuck, and A. Tohsaki, Phys. Rev. C **85**, 034315 (2012).
[45] T. Ichikawa, N. Itagaki, Y. Kanada-En'yo, T. Kokalova, and W. Von Oertzen, Phys. Rev. C **86**, 031303(R) (2012).
[46] Z. H. Yang, Y. L. Ye, Z. H. Li, J. L. Lou, J. S. Wang, D. X. Jiang, Y. C. Ge, Q. T. Li, H. Hua, X. Q. Li, F. R. Xu, J. C. Pei *et al.*, Phys. Rev. Lett. **112**, 162501 (2014).
[47] Y. Kanada-En'yo, Phys. Rev. C **89**, 024302 (2014).
[48] T. Yamada and Y. Funaki, Phys. Rev. C **92**, 034326 (2015).
[49] Y. Chiba and M. Kimura, Phys. Rev. C **91**, 061302(R) (2015).
[50] Y. Chiba, Y. Taniguchi, and M. Kimura, Phys. Rev. C **95**, 044328 (2017).
[51] M. Nakao, H. Umehara, S. Ebata, and M. Ito, Phys. Rev. C **98**, 054318 (2018).
[52] Y. Kanada-En'yo and Y. Shikata, Phys. Rev. C **100**, 014301 (2019).
[53] Y. Chiba and M. Kimura, Phys. Rev. C **101**, 024317 (2020).
[54] Y. Kanada-En'yo and K. Ogata, Phys. Rev. C **101**, 014317 (2020).
[55] T. Baba and M. Kimura, Phys. Rev. C **102**, 024317 (2020).
[56] M. Itoh, S. Kishi, H. Sakaguchi, H. Akimune, M. Fujiwara, U. Garg, K. Hara, H. Hashimoto, J. Hoffman, T. Kawabata, K. Kawase, T. Murakami, K. Nakanishi, B. K. Nayak, S. Terashima, M. Uchida, Y. Yasuda, and M. Yosoi, Phys. Rev. C **88**, 064313 (2013).
[57] Y. Kanada-En'yo, M. Kimura, and H. Horiuchi, C. R. Phys. **4**, 497 (2003).
[58] Y. Kanada-En'yo, M. Kimura, and A. Ono, Prog. Theor. Exp. Phys. **2012**, 1A202 (2012).
[59] M. Kimura, T. Suhara, and Y. Kanada-En'yo, Eur. Phys. J. A **52**, 373 (2016).
[60] Y. Kanada-En'yo and M. Kimura, Phys. Rev. C **72**, 064322 (2005).
[61] M. Kimura and H. Horiuchi, Nucl. Phys. A **767**, 58 (2006).
[62] Y. Taniguchi, M. Kimura, Y. Kanada-En'yo, and H. Horiuchi, Phys. Rev. C **76**, 044317 (2007).
[63] Y. Taniguchi, Y. Kanada-En'yo, and M. Kimura, Phys. Rev. C **80**, 044316 (2009).
[64] Y. Taniguchi and M. Kimura, Phys. Lett. B **800**, 135086 (2020).
[65] J. Berger, M. Girod, and D. Gogny, Comput. Phys. Commun. **63**, 365 (1991).
[66] M. Kimura, Phys. Rev. C **69**, 044319 (2004).
[67] Y. Taniguchi, M. Kimura, and H. Horiuchi, Prog. Theor. Phys. **112**, 475 (2004).
[68] D. L. Hill and J. A. Wheeler, Phys. Rev. **89**, 1102 (1953).
[69] Y. Chiba and M. Kimura, Prog. Theor. Exp. Phys. **2017**, 053D01 (2017).
[70] H. Horiuchi, Prog. Theor. Phys. **47**, 1058 (1972).
[71] H. Horiuchi, Prog. Theor. Phys. Suppl. **62**, 90 (1977).
[72] R. R. Rodríguez-Guzmán, J. L. Egido, and L. M. Robledo, Phys. Rev. C **62**, 054308 (2000).
[73] T. Inakura, S. Mizutori, M. Yamagami, and K. Matsuyanagi, Nucl. Phys. A **710**, 261 (2002).
[74] M. Bender, H. Flocard, and P. H. Heenen, Phys. Rev. C **68**, 044321 (2003).
[75] N. Curtis, A. S. J. Murphy, N. M. Clarke, M. Freer, B. R. Fulton, S. J. Hall, M. J. Leddy, J. S. Pople, G. Tungate, R. P. Ward, W. N. Catford, G. J. Gyapong, S. M. Singer, S. P. G. Chappell, S. P. Fox, C. D. Jones, D. L. Watson, W. D. M. Rae, P. M. Simmons, and P. H. Regan, Phys. Rev. C **53**, 1804 (1996).
[76] B. Bayman and A. Bohr, Nucl. Phys. **9**, 596 (1958).
[77] T. A. Carey, P. G. Roos, N. S. Chant, A. Nadasen, and H. L. Chen, Phys. Rev. C **29**, 1273 (1984).
[78] P. G. Roos, N. S. Chant, A. A. Cowley, D. A. Goldberg, H. D. Holmgren, and R. Woody, Phys. Rev. C **15**, 69 (1977).
[79] T. Yoshimura, A. Okihana, R. E. Warner, N. S. Chant, P. G. Roos, C. Samanta, S. Kakigi, N. Koori, M. Fujiwara, N. Matsuoka, K. Tamura, E. Kubo, and K. Ushiro, Nucl. Phys. A **641**, 3 (1998).
[80] K. Yoshida, K. Minomo, and K. Ogata, Phys. Rev. C **94**, 044604 (2016).
[81] K. Yoshida, K. Ogata, and Y. Kanada-En'yo, Phys. Rev. C **98**, 024614 (2018).
[82] K. Yoshida, Y. Chiba, M. Kimura, Y. Taniguchi, Y. Kanada-En'yo, and K. Ogata, Phys. Rev. C **100**, 044601 (2019).
[83] A. S. Reiner, Nucl. Phys. **27**, 115 (1961).
[84] C. Ouellet and B. Singh, Nucl. Data Sheets **112**, 2199 (2011).
[85] R. B. Leachman, P. Fessenden, and W. R. Gibbs, Phys. Rev. C **6**, 1240 (1972).
[86] A. W. Obst and K. W. Kemper, Phys. Rev. C **6**, 1705 (1972).